Synthesis and Structural Relationship of the Ternary Indides $Sc_3Ni_{2.10(5)}In_{3.60(5)}$, $Sc_3Ni_{2.14(2)}In_{3.76(2)}$, $ScPd_{0.981(2)}In$ and $Sc_3Rh_{1.594(9)}In_4$

Mar'yana Lukachuk[a], Vasyl' I. Zaremba[a,b], Rolf-Dieter Hoffmann[a], and Rainer Pöttgen[a]

[a] Institut für Anorganische und Analytische Chemie and NRW Graduate School of Chemistry, Westfälische Wilhelms-Universität Münster, Wilhelm-Klemm-Strasse 8, 48149 Münster, Germany
[b] Inorganic Chemistry Department, Ivan Franko National University of Lviv, Kyryla and Mephodiya Street 6, 79005 Lviv, Ukraine

Reprint requests to R. Pöttgen. E-mail: pottgen@uni-muenster.de

Z. Naturforsch. **59b,** 182 – 189 (2004); received December 12, 2003

Dedicated to Professor Ingo-Peter Lorenz on the occasion of his 60th birthday

The ternary scandium transition metal indides $Sc_3Ni_{2.10(5)}In_{3.60(5)}$, $Sc_3Ni_{2.14(2)}In_{3.76(2)}$, $ScPd_{0.981(2)}In$, and $Sc_3Rh_{1.594(9)}In_4$ have been synthesized from the elements in glassy carbon crucibles in a high frequency furnace or by arc-melting. They have been investigated by X-ray powder diffraction and the structures refined on the basis of single crystal diffractometer data: $Lu_3Co_{1.87}In_4$ type, $P\bar{6}$, $a = 745.7(1)$, $c = 342.85(7)$ pm, $wR2 = 0.0689$, 545 F^2, 24 parameters for $Sc_3Ni_{2.10(5)}In_{3.60(5)}$, $a = 753.63(7)$, $c = 344.3(1)$ pm, $wR2 = 0.0362$, 792 F^2, 22 parameters for $Sc_3Ni_{2.14(2)}In_{3.76(2)}$, $P\bar{6}2m$, ZrNiAl type, $a = 764.1(2)$, $c = 345.90(8)$ pm, $wR2 = 0.0333$, 326 F^2, 15 parameters for $ScPd_{0.981(2)}In$, and $P\bar{6}$, $a = 769.4(1)$, $c = 684.1(1)$ pm, $wR2 = 0.0526$, 1097 F^2, 35 parameters for the new structure type $Sc_3Rh_{1.594(9)}In_4$. In the three structure types the scandium atoms build trigonal prisms. The latter are filled exclusively by palladium atoms in $ScPd_{0.981(2)}In$, while transition metal and indium atoms fill these sites in the other three structures. The different coloring of the trigonal prismatic sites leads to a symmetry reduction for the structures of $Sc_3Ni_{2.10(5)}In_{3.76(5)}$, $Sc_3Ni_{2.14(2)}In_{3.76(2)}$ and $Sc_3Rh_{1.594(9)}In_4$. The structural relationship is described on the basis of a group-subgroup scheme. Chemical bonding in these intermetallics is briefly discussed.

Key words: Indium, Crystal Structure, Scandium

Introduction

The ternary systems rare earth metal-transition metal-indium have intensively been investigated in recent years with respect to phase analyses, crystal chemistry, and physical properties. The structural chemistry and an overview of the magnetic and electrical properties are given in three recent reviews [1 – 3]. In many isostructural series, also the respective compounds with yttrium exist. The metallic radius of yttrium (181 pm) is close to that of gadolinium (180 pm) [4]. Consequently, the cell volumes of the ternary yttrium-transition metal-indides fit between those of the corresponding gadolinium and terbium, or terbium and dysprosium compounds [3]. Yttrium shows some flexibility and reacts on the geometrical requirements of the transition metal-indium network. In the case of some ternary carbides and phosphides, the cell volume of the yttrium compound even fits in between those of the dysprosium and holmium compounds [5 – 7].

Scandium, however, which has a significantly smaller metallic radius of 161 pm [4] sometimes also forms an isotypic compound within the rare earth metal series. This leads in some cases to drastic changes in chemical bonding. In metal rich compounds the Sc–Sc bonding might be more pronounced, *e. g.* ScNiP [8]. Other rare earth compounds show pronounced changes in the polyanionic networks, *e. g.* two-dimensional [AuGe] networks in CeAuGe and LuAuGe, but a three-dimensional one in ScAuGe [9].

The ternary systems scandium-transition metal-indium have so far only scarcely been investigated [10]. $ScNi_4In$ ($MgCu_4Sn$ type) [11], ScT_2In (T = Ni, Cu, Pd, Ag, Pt, Au) ($MnCu_2Al$ type) [12 – 14], Sc_2T_2In (T = Ni, Cu, Pd, Au) (Mo_2FeB_2 or U_2Pt_2

Table 1. Crystal data and structure refinement for $ScPd_{0.981(2)}In$, $Sc_3Ni_{2.10(5)}In_{3.60(5)}$, $Sc_3Ni_{2.14(2)}In_{3.76(2)}$, $Sc_3Rh_{1.594(9)}In_4$.

Empirical formula	$ScPd_{0.981(2)}In$	$Sc_3Ni_{2.10(5)}In_{3.60(5)}$	$Sc_3Ni_{2.14(2)}In_{3.76(2)}$	$Sc_3Rh_{1.594(9)}In_4$
Molar mass	264.05 g/mol	671.52 g/mol	692.24 g/mol	758.31 g/mol
Structure type	ZrNiAl	$Lu_3Co_{1.87}In_4$	$Lu_3Co_{1.87}In_4$	new structure type
Space group, Z	$P\bar{6}2m$, 3	$P6$, 1	$P6$, 1	$P6$, 2
Unit cell dimensions	$a = 764.1(2)$ pm	$a = 745.7(1)$ pm	$a = 753.63(7)$ pm	$a = 769.4(1)$ pm
	$c = 345.90(8)$ pm	$c = 342.85(7)$ pm	$c = 344.3(1)$ pm	$c = 684.1(1)$ pm
	V= 0.1749 nm^3	V= 0.1651 nm^3	V= 0.1694 nm^3	V= 0.3507 nm^3
Calculated density	7.52 g/cm^3	6.75 g/cm^3	6.79 g/cm^3	7.18 g/cm^3
Crystal size	$20 \times 20 \times 40$ μm^3	$20 \times 30 \times 50$ μm^3	$20 \times 20 \times 40$ μm^3	$10 \times 40 \times 40$ μm^3
Detector distance	60 mm	60 mm	–	60 mm
Exposure time	30 min	40 min	–	20 min
ω Range; increment	0 – 180°; 1.0°	0 – 180°; 1.0°	–	0 – 180°; 1.0°
Integr. param. A, B, EMS	14.5; 4.5; 0.012	14.0; 3.5; 0.022	–	15.0; 4.5; 0.020
Transm. ratio (max/min)	1.24	1.63	1.42	1.36
Absorption coefficient	19.7 mm^{-1}	20.9 mm^{-1}	21.0 mm^{-1}	19.1 mm^{-1}
$F(000)$	345	298	307	662
θ range	3° to 35°	3° to 35°	3° to 40°	3° to 35°
Range in hkl	$-11 \le h \le 12$, ± 12, ± 5	± 11, ± 11, ± 5	± 13, ± 13, ± 6	± 12, $-12 \le k \le 11$, ± 10
Total no. reflections	2703	2446	4215	5261
Independent reflections	326($R_{int} = 0.0416$)	545($R_{int} = 0.0549$)	792($R_{int} = 0.0543$)	1097($R_{int} = 0.0369$)
Reflections with $I > 2\sigma(I)$	315($R_\sigma = 0.0194$)	522($R_\sigma = 0.0314$)	759($R_\sigma = 0.0292$)	894($R_\sigma = 0.0241$)
Data/parameters	326 / 15	545 / 24	792 / 22	1097 / 35
Goodness-of-fit on F^2	1.124	1.213	1.115	1.144
Final R indices	$R1 = 0.0171$	$R1 = 0.0258$	$R1 = 0.0201$	$R1 = 0.0311$
$[I > 2\sigma(I)]$	$wR2 = 0.0331$	$wR2 = 0.0541$	$wR2 = 0.0356$	$wR2 = 0.0496$
R Indices (all data)	$R1 = 0.0183$	$R1 = 0.0289$	$R1 = 0.0230$	$R1 = 0.0438$
	$wR2 = 0.0333$	$wR2 = 0.0689$	$wR2 = 0.0362$	$wR2 = 0.0526$
Flack parameter	0.06(13)	0.01(11)	−0.03(4)	0.06(10)
Extinction coefficient	0.007(1)	0.029(3)	0.045(1)	0.0067(3)
Largest diff.	0.66 and	1.16 and	1.92 and	2.85 and
peak and hole	−0.97 e/Å^3	−1.47 e/Å^3	−1.64 e/Å^3	−2.32 e/Å^3

Sn type) [15, 16], ScPtIn with ZrNiAl structure [17], and a solid solution $Sc_{1-x}PdIn_x$ [18] with CsCl structure have been reported. We have now started a systematic investigation of the scandium-transition metal-indium systems with respect to phase analyses, crystal chemistry, and chemical bonding peculiarities. Herein we report on the synthesis and structural characterization of the two nickel indides $Sc_3Ni_{2.10(5)}In_{3.60(5)}$, $Sc_3Ni_{2.14(2)}In_{3.76(2)}$, $ScPd_{0.981(2)}In$, and $Sc_3Rh_{1.594(9)}In_4$.

Experimental Section

Synthesis

Starting materials for the preparation of the title compounds were scandium ingots (Kelpin), nickel wire (⌀ 0.38 mm, Johnson Matthey), rhodium and palladium powder (*ca.* 200 mesh, Degussa-Hüls), and indium tear drops (Johnson Matthey), all with purities better than 99.9%. Smaller pieces of scandium were prepared by mechanical fragmentation of the larger ingot. The scandium pieces were arc-melted [19] in a first step under argon. This pre-melting procedure avoids shattering during the subsequent reactions with the other elements. The argon was purified over molecular sieves, silica gel, and titanium sponge (900 K).

$ScPd_{0.981}In$ was prepared by arc-melting of the elements in the ideal 1:1:2 atomic ratio under an argon atmosphere of about 800 mbar. The button was remelted three times to ensure homogeneity and subsequently sealed in an evacuated quartz tube and annealed at 1070 K for four weeks.

The first nickel compound $Sc_3Ni_{2.10}In_{3.60}$ originated from a sample prepared by arc-melting of the elements in the atomic ratio 1:1:2. The sample was homogenized by two subsequent melting procedures. The weight losses due to evaporations and shattering were smaller than 0.5%. The sample was enclosed in an evacuated silica ampoule, first heated for 40 h at 1300 K, followed by slow cooling to 1070 K at a rate of 5 K/h and then to 770 K at a rate of 15 K/h. Finally the sample was quenched by radiative heat loss inside the furnace.

The second nickel containing sample, leading to $Sc_3Ni_{2.14}In_{3.76}$ was synthesized by high-frequency melting (Hüttinger Elektronik, Freiburg, Typ TIG 1.5/300) of the elements in the 5:2:4 atomic ratio in a glassy carbon crucible (SIGRADUR®G, glassy carbon, type GAZ006) under flowing argon. This sample was first heated for half a minute at about 1300 K, cooled to about 1100 K, heated again to 1300 K and finally annealed at about 900 K for another two hours. The rhodium containing sample was obtained with the same temperature program but with the starting composition Sc:Rh:In = 3:2:4.

All samples were obtained in amounts of about 1 g. Compact pieces are light grey with metallic lustre. The samples

Table 2. Atomic coordinates and isotropic displacement parameters (pm^2) for $ScPd_{0.981(2)}In$, $Sc_3Ni_{2.10(5)}In_{3.60(5)}$, $Sc_3Ni_{2.14(2)}In_{3.76(2)}$ and $Sc_3Rh_{1.594(9)}In_4$. U_{eq} is defined as one third of the trace of the orthogonalized U_{ij} tensor. The M positions show mixed Ni/In occupancy.

Atom	Wyckoff position	Occupancy, %	*x*	*y*	*z*	U_{eq}
$ScPd_{0.981(2)}In$ (space group *P*$\bar{6}$2*m*)						
Sc	3*f*	100	0.6051(2)	0	0	173(3)
Pd1	2*d*	100	1/3	2/3	1/2	143(1)
Pd2	1*a*	94.2(6)	0	0	0	120(3)
In	3*g*	100	0.27073(6)	0	1/2	129(1)
$Sc_3Ni_{2.10(5)}In_{3.60(5)}$ (space group *P*$\bar{6}$)						
Sc	3*j*	100	0.4126(9)	0.017(2)	0	267(10)
Ni1	1*a*	70(1)	0	0	0	146(9)
M1	1*f*	76(5) Ni / 24(5) In	2/3	1/3	1/2	166(16)
M2	1*d*	65(5) Ni / 35(5) In	1/3	2/3	1/2	125(13)
In2	3*k*	100	0.7441(2)	0.9996(4)	1/2	177(2)
$Sc_3Ni_{2.14(2)}In_{3.76(2)}$ (space group *P*$\bar{6}$)						
Sc	3*j*	100	0.4136(2)	0.0316(2)	0	137(2)
Ni1	1*a*	90.5(6)	0	0	0	103(3)
Ni2	1*f*	100	2/3	1/3	1/2	98(2)
M	1*d*	23.9(9) Ni / 76.1(9) In	1/3	2/3	1/2	99(2)
In2	3*k*	100	0.7407(1)	0.00086(5)	1/2	112(1)
$Sc_3Rh_{1.594(9)}In_4$ (space group *P*$\bar{6}$)						
Sc1	3*j*	100	0.4214(4)	0.0353(4)	0	140(4)
Sc2	3*k*	100	0.4106(4)	0.0414(4)	1/2	125(4)
Rh1	1*a*	41.2(9)	0	0	0	104(10)
Rh2	1*b*	77.5(9)	0	0	1/2	87(5)
Rh3	2*i*	100	2/3	1/3	0.7505(2)	85(1)
In1	2*h*	100	1/3	2/3	0.7370(2)	128(2)
In2	6*l*	100	0.74341(7)	0.99711(7)	0.7601(1)	165(1)

are stable in moist air. No decomposition was observed after several weeks.

EDX analyses

The samples and the single crystals investigated on the diffractometers were analyzed with a LEICA 420 I scanning electron microscope using Sc, Ni, Rh, Pd, and InAs as standards. No metallic impurity elements were detected. Within 2 at.-%, the compositions determined via EDX agreed with the compositions refined from the single crystal X-ray data.

X-ray investigations

The samples were characterized through Guinier powder patterns using Cu-$K_{\alpha 1}$ radiation and α-quartz (a = 491.30, c = 540.46 pm) as an internal standard. The Guinier camera was equipped with an imaging plate system (Fujifilm-BAS-1800). The hexagonal lattice parameters (Table 1) were obtained from least-squares fits of the powder data. To ensure correct indexing, the experimental patterns were compared with calculated ones [20] taking the atomic positions obtained from the structure refinements. For $ScPd_{0.981(2)}In$ and $Sc_3Rh_{1.594(9)}In_4$, the lattice parameters determined for the powders and the single crystals agreed well. For the nickel containing samples the powder and single crystal data showed slight differences. We therefore calculated the interatomic distances with the single crystal lattice parameters. The powder lattice parameters were a = 754.8(4), c = 344.9(2) pm for the sample from the 1:1:2 starting composition and a = 746.9(3), c = 343.2(1) pm for the one with the 5:2:4 starting composition. The powder pattern of the 1:1:2 sample showed elemental indium as a second phase. For $Sc_3Rh_{1.594(9)}In_4$, the very weak superstructure reflections were not visible on the Guinier powder pattern. The strongest calculated superstructure reflection had only 2.8% intensity, when compared with the strongest subcell reflection.

Irregularly shaped single crystals of the four indides were selected from the crushed samples. They were first examined by Laue photographs on a Buerger precession camera (Mo-K_α radiation) equipped with an image plate system (Fujifilm BAS-1800) in order to establish suitability for intensity data collection. Single crystal intensity data of $Sc_3Ni_{2.14(2)}In_{3.76(2)}$ were collected on a four-circle diffractometer (Nonius, CAD4) with graphite monochromatized Mo-K_α radiation (71.073 pm) and a scintillation counter with pulse height discrimination. Scans were taken in the $\omega/2\theta$ mode and an empirical absorption correction was applied on the basis of psi-scan data followed by a spherical absorption correction. Intensity data of the other crystals were collected on a Stoe IPDS-II diffractometer in oscillation mode also with graphite monochromatized Mo-K_α radiation. All relevant parameters for the data collections are listed in Table 1.

Structure refinements

The structure of the palladium compound was refined first. The atomic parameters of ScPtIn [17] were taken as

$ScPd_{0.981(2)}In$				$Sc_3Ni_{2.10(5)}In_{3.60(5)}$				$Sc_3Ni_{2.14(2)}In_{3.76(2)}$				$Sc_3Rh_{1.594(9)}In_4$			
Sc:	4	Pd1	291.6(1)	Sc:	2	M1	276.2(8)	Sc:	2	Ni2	272.7(1)	Sc1:	2	Rh3	272.2(2)
	1	Pd2	301.7(2)		2	M2	292.6(8)		1	Ni1	300.5(1)		2	In2	307.4(3)
	2	In	308.5(2)		1	Ni1	301.6(3)		2	M	303.8(1)		2	In2	310.6(2)
	4	In	318.3(1)		2	In2	306.3(2)		2	In2	303.8(1)		1	Rh1	311.5(3)
	2	Sc	345.9(1)		2	In2	309.5(6)		2	In2	310.9(1)		2	In1	313.4(2)
Pd1:	3	In	281.7(1)		2	In2	320.5(7)		2	In2	326.9(1)		2	In2	329.3(2)
	6	Sc	291.6(1)		2	Sc	342.9(1)		2	Sc	344.3(1)		2	Sc2	342.2(1)
Pd2:	6	In	269.6(1)		2	Sc	375.0(17)		2	Sc	366.3(2)		2	Sc1	367.1(5)
	3	Sc	301.7(2)	Ni1:	6	In2	256.4(1)	Ni1:	6	In2	260.7(1)	Sc2:	2	Rh3	272.7(2)
In:	2	Pd2	269.6(1)		3	Sc	301.6(3)		3	Sc	300.5(1)		1	Rh2	301.3(3)
	2	Pd1	281.7(1)	M1:	6	Sc	276.2(8)	Ni2:	6	Sc	272.7(1)		2	In2	306.0(2)
	2	Sc	308.5(2)		3	In2	282.2(2)		3	In2	282.6(1)		2	In1	309.5(2)
	4	Sc	318.3(1)	M2:	3	In2	281.8(2)	M:	3	In2	283.5(1)		2	In2	327.3(2)
	2	In	345.9(1)		6	Sc	292.6(8)		6	Sc	303.8(1)		2	In2	332.3(2)
	2	In	358.3(1)		2	M2	342.9(1)		2	M	344.3(1)		2	Sc1	342.2(1)
				In2:	2	Ni1	256.4(1)	In2:	2	Ni1	260.7(1)		2	Sc2	367.5(4)
					1	M2	281.8(2)		1	Ni2	282.6(1)	Rh1:	6	In2	255.9(1)
					1	M1	282.2(2)		1	M	283.5(1)		3	Sc1	311.5(3)
					2	Sc	306.3(2)		2	Sc	303.8(1)	Rh2:	6	In2	265.0(1)
					2	Sc	309.5(6)		2	Sc	310.9(1)		3	Sc2	301.3(3)
					2	Sc	320.5(7)		2	Sc	326.9(1)	Rh3:	3	Sc1	272.2(2)
					2	In2	330.3(1)		2	In2	339.0(1)		3	Sc2	272.7(2)
					2	In2	342.9(1)		2	In2	344.3(1)		3	In2	292.8(1)
												In1:	3	In2	290.2(1)
													3	Sc2	309.5(2)
													3	Sc1	313.4(2)
													1	In1	324.3(2)
													1	In1	359.8(2)
												In2:	1	Rh1	255.9(1)
													1	Rh2	265.0(1)
													1	In1	290.2(1)
													1	Rh3	292.8(1)
													1	Sc2	306.0(2)
													1	Sc1	307.4(3)
													1	Sc1	310.6(2)
													1	Sc2	327.3(2)
													1	In2	328.2(1)
													1	Sc1	329.3(2)
													1	Sc2	332.3(2)
													2	In2	340.0(1)
													1	In2	355.9(1)

Table 3. Interatomic distances (pm), calculated with the lattice parameters taken from X-ray single crystal data of $Sc_3Ni_{2.10(5)}In_{3.60(5)}$ and $Sc_3Ni_{2.14(2)}In_{3.76(2)}$. The distances for $ScPd_{0.981(2)}In$ and $Sc_3Rh_{1.594(9)}In_4$ have been calculated with the powder lattice parameters. All distances within the first coordination spheres are listed. The M position shows mixed Ni/In occupancy (see Table 2).

starting values and the structure was successfully refined using SHELXL-97 [21] with anisotropic displacement parameters for all atoms. Refinement of the correct absolute structure was ensured through refinement of the Flack parameter [22, 23]. In a separate series of least-squares cycles, the occupancy parameters were refined as a check for the correct composition. The Sc, Pd1, and In sites were fully occupied within two standard deviations, while the Pd2 site had a smaller occupancy. In the final cycles the ideal occupancies were assumed for Sc, Pd1, and In, while the occupancy parameter of Pd2 was refined as a least-squares variable, leading to the composition $ScPd_{0.981(2)}In$ for the crystal investigated.

Refinement of the nickel data sets with the model of the palladium compound failed. Careful analysis of the data sets revealed low hexagonal Laue symmetry and no systematic extinctions, leading to space groups $P6/m$, $P\bar{6}$, and $P6$, of which $P\bar{6}$ was found to be correct during the structure refinements.

Lowering of the space group symmetry from $P\bar{6}2m$ to $P\bar{6}$ *via* a *translationengleiche* symmetry reduction of index 2 (t2) leads to a splitting of the 2*d* Pd1 site into two one-fold sites 1*d* and 1*f* as shown in the Bärnighausen tree [24, 25] in Fig. 1. Furthermore, the Sc and In atoms gain a variable *y* parameter. We then transformed the atomic parameters to the setting of space group $P\bar{6}$. In the first refinement cycles, all three one-fold positions were refined with nickel atoms. For both crystals we found full occupancy for the scandium and indium sites, but different behavior for the one-fold sites. The first crystal showed only 70% Ni occupancy on the 1*a* site

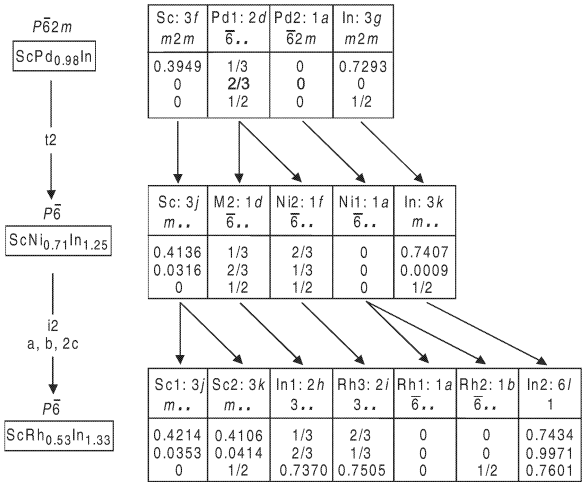

Fig. 1. Group-subgroup scheme in the Bärnighausen formalism [24, 25] for the structures of $ScPd_{0.981(2)}In$, $ScNi_{0.71}In_{1.25}$ (*i.e.* $Sc_3Ni_{2.14(2)}In_{3.76(2)}$) and $ScRh_{0.53}In_{1.33}$ (*i.e.* $Sc_3Rh_{1.594(9)}In_4$). The indices of the *translationengleiche* (t) and isomorphic (i) transitions, as well as the unit cell transformation are given. The evolution of the atomic parameters is shown at the right-hand part. The $ScPd_{0.981(2)}In$ structure is presented here in the setting of the opposite absolute structure.

and different Ni/In ratios on the sites 1*d* and 1*f*. Furthermore this crystal showed meroedric twinning through the twin matrix $(0\bar{1}0\,100\,00\bar{1})$. With the symmetry reduction from $P\bar{6}2m$ to $P\bar{6}$ the mirror planes and the two-fold axes are lost. The latter can be taken as the twinning element for this crystal. The second crystal was not twinned and the 1*f* site showed full occupancy with nickel, but only 91% nickel occupancy on the 1*a* site. Again, there was Ni/In mixing for the 1*d* site. Although the crystals have similar compositions, the site occupancies differ significantly (Table 2).

The rhodium based crystal showed doubling of the subcell *c* axis in the IPDS-II data set. Analysis of the data set showed low Laue symmetry, and consequently, in going from the subcell space group $P\bar{6}$, the next step of symmetry reduction is an isomorphic transition of index 2 (i2) to $P\bar{6}$ upon doubling the *c* axis. As emphasized in Fig. 1, now also the Sc and the Ni1 positions split into two crystallographically independent sites. This allows ordering on the two transition metal positions and furthermore, both scandium sites show different *x* and *y* parameters, leading to different sizes for the trigonal prisms. Refinement of the occupancy parameters of the Rh1 and Rh2 sites showed significant defects on these positions. Both occupancy parameters were refined as a least-squares variable in the final cycles. The crystal chemical reason for this behavior is discussed below.

Final difference Fourier synthesis for all data sets showed no significant residual peaks (Table 1). The resulting residuals are listed in Table 1, the positional parameters in Table 2, and the interatomic distances in Table 3. Listings of the anisotropic displacement parameters and the observed and calculated structure factors are available.*

Discussion

The four new scandium transition metal indides $ScPd_{0.981(2)}In$, $Sc_3Ni_{2.10(5)}In_{3.60(5)}$, $Sc_3Ni_{2.14(2)}In_{3.76(2)}$, and $Sc_3Rh_{1.594(9)}In_4$ reported herein crystallize with different ordered versions of the binary Fe_2P [26] type. An overview of the different site occupancy variants and superstructures of the Fe_2P type has been given recently [27–29].

$ScPd_{0.981(2)}In$ crystallizes with the ZrNiAl type structure [30–32]. A projection is shown in Fig. 2. The indium atoms build trigonal prisms around the origin of the unit cell. These prisms are filled with the Pd1 atoms and they are condensed along the *c* axis *via* the triangular faces. The scandium atoms also form trigonal prisms. The latter are filled by the Pd2 atoms and they are condensed *via* common edges forming six-membered rings around the prisms of the indium atoms. The Pd2 position shows only an occupancy of 94.2(6)%. This is correlated with the shorter Pd2-In distances of 270 pm as compared to Pd1-In (282 pm). The Pd2-In distances are shorter than the sum of the covalent radii of 278 pm [4]. Based on the comparison of the interatomic distances, the Pd-In interactions seem to be the strongest ones in the $ScPd_{0.981(2)}In$ structure.

The coloring of the trigonal prisms by transition metal and indium atoms is different in the nickel containing compounds. Here, the indium atoms also form prisms around the origin (Fig. 2). These are occupied by Ni at 70% in $Sc_3Ni_{2.10(5)}In_{3.60(5)}$ and at 91% in $Sc_3Ni_{2.14(2)}In_{3.76(2)}$. The lower occupancy in the first compound can be understood by the shorter Ni1-In2 distances of 256 pm as compared to 261 pm in $Sc_3Ni_{2.14(2)}In_{3.76(2)}$. Within the six-membered rings of the trigonal prisms formed by scandium, we observe occupancy by three Ni2 atoms and by a Ni/In mixture in the other three remaining prisms in

*Details may be obtained from: Fachinformationszentrum Karlsruhe, D-76344 Eggenstein-Leopoldshafen (Germany), by quoting the Registry No's. CSD–413567 ($ScPd_{0.981}In$), CSD-413566 ($Sc_3Ni_{2.10}In_{3.60}$), CSD-413565 ($Sc_3Ni_{2.14}In_{3.76}$), and CSD-413568 ($Sc_3Rh_{1.594}In_4$). E-mail: crysdata@FIZ-Karlsruhe.de.

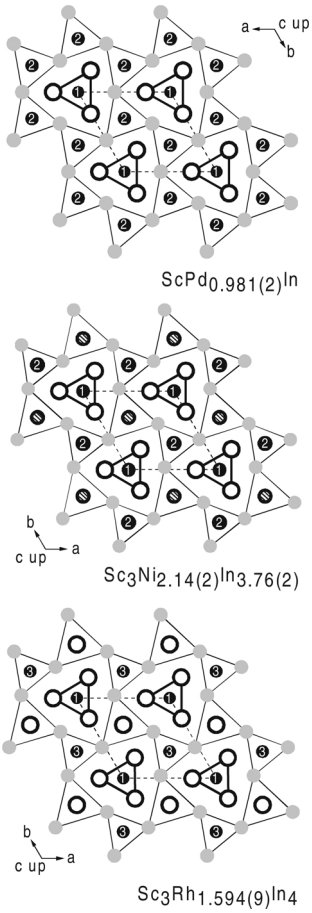

Fig. 2. Projections of the $ScPd_{0.981(2)}In$, $Sc_3Ni_{2.14(2)}In_{3.76(2)}$, and $Sc_3Rh_{1.594(9)}In_4$ structures along the *c* axis. Scandium, transition metal, and indium atom are drawn as light grey, filled, and open circles, respectively. The mixed Ni/In site in $Sc_3Ni_{2.14(2)}In_{3.76(2)}$ is drawn with shaded circles. The trigonal prisms formed by the indium and scandium atoms are emphasized. For clarity, only half the unit cell is shown for the rhodium compound. The crystallographically different transition metal sites are indicated.

$Sc_3Ni_{2.14(2)}In_{3.76(2)}$. In the $Sc_3Ni_{2.10(5)}In_{3.60(5)}$ structure, all positions in the scandium prisms show mixed Ni/In occupancies. This coloring is similar to the $Lu_3Co_{1.87}In_4$ structure [33], but with slightly differing occupancies. Due to the variable *y* parameter in space group $P\bar{6}$, the scandium atoms can shift and vary the size of the prisms and thus react on the different size of the atoms within the prisms.

$Sc_3Rh_{1.594(9)}In_4$ crystallizes with a new superstructure of the Fe_2P family. The image plate data revealed

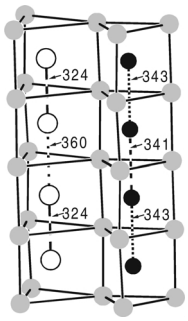

Fig. 3. Cutout of the $Sc_3Rh_{1.594(9)}In_4$ structure. Scandium, rhodium, and indium atoms are drawn as light grey, filled, and open circles, respectively. Some rows of trigonal prismatic units together with relevant interatomic distances are indicated in units of pm.

a doubling of the *c* lattice parameter and also showed low Laue symmetry. Thus, $Sc_3Rh_{1.594(9)}In_4$ crystallizes in the isomorphic subgroup $P\bar{6}$ of index 2 (i2) of $P\bar{6}$. Referring to the subcell in space group $P62m$, only the indium atoms don't show a splitting of the sites, however, they obtain variable *y* and *z* parameters in the superstructure. In contrast to the structures of the nickel compounds, we observe no mixed occupancies in the rhodium compound. Nevertheless, the Rh1 and Rh2 sites show defects. Again, these are correlated with the Rh-In distances.

At this point it is worthwhile to compare the $Sc_3Rh_{1.594(9)}In_4$ structure with the structures of $Ti_3Rh_2In_3$ [34], $ZrRh_{0.710(4)}In$ [35], and TmRhIn [36]. All of them crystallize with a Fe_2P related structure. In $Ti_3Rh_2In_3$ [34], the trigonal prisms at the origin of the unit cell all remain empty. This is due to the small titanium atoms. If a rhodium atom would occupy this position, an unreasonably short Rh-In distance of 231 pm would result. In $ZrRh_{0.710(4)}In$ [35] with the slightly larger zirconium atom, this position is filled with 12% rhodium, resulting in a Rh-In distance of 243 pm. In $Sc_3Rh_{1.594(9)}In_4$, reported herein, the Rh1 and Rh2 sites have occupancy parameters of 41 and 78% with Rh1-In and Rh2-In distances of 256 and 265 pm. In TmRhIn [36] the rhodium site is fully occupied with a Rh1-In distance of 271 pm. For comparison, the sum of the covalent radii is 275 pm [4]. Thus, the occupancy parameter of the rhodium sites nicely scales with the size of the trigonal prisms and the Rh-In distances.

The above result is actually not understandable looking at a local spot in a structure. A lower occu-

pancy does not resolve the occurrence of too short distances. This dilemma, however, is resolved by taking into account that locally strain might occur and, thus, the atoms are squeezed in. For the whole crystal, however, the sum of all the local strain limits the total occupancies.

Within the scandium based prisms, we observe an occupancy by In1 and Rh3 atoms. Since these atoms differ significantly in size, the scandium atoms also react with a small displacement. In Fig. 3 we present a cutout of the trigonal prismatic scandium units. The indium atoms are dislocated from the subcell mirror plane, forming In_2 pairs at In1-In1 distances of 324 pm, close to the In-In distances in elemental indium (tetragonal body-centered structure, 4×325 and 8×338 pm In-In [37]). Thus, the $Sc_3Rh_{1.594(9)}In_4$ structure is also dominated by strong Rh-In and In-In interactions.

Summing up, we observe four scandium transition metal indides, which crystallize with a different coloring of the transition metal and indium atoms. The four structures are governed by strongly bonding *T*-In and In-In interactions, while Sc-Sc bonding plays a minor role. The shortest Sc-Sc distances range between 342 and 346 pm, longer than the average Sc-Sc distance of 328 pm in *hcp* scandium. The crystal chemistry of these four intermetallics can be understood on the basis of a group-subgroup scheme.

Acknowledgments

We thank Dipl.-Ing. U. Ch. Rodewald for the intensity data collections and H.-J. Göcke for the work at the scanning electron microscope. This work was financially supported by the Fonds der Chemischen Industrie and by the Deutsche Forschungsgemeinschaft. M. L. is indebted to the NRW Graduate School of Chemistry for a PhD stipend.

[1] Ya. M. Kalychak, J. Alloys Compd. **262**, 341 (1997).
[2] Ya. M. Kalychak, J. Alloys Compd. **291**, 80 (1999).
[3] Ya. M. Kalychak, V. I. Zaremba, R. Pöttgen, M. Lukachuk, R.-D. Hoffmann, Rare Earth-Transition Metal-Indides, in K. A. Gschneider (Jr.), V. K. Pecharsky, J.-C. Bünzli (eds.): Handbook on the Physics and Chemistry of Rare Earths, Elsevier, Amsterdam (2003), in press.
[4] J. Emsley, The Elements, 3rd edn, Oxford University Press, Oxford (1999).
[5] W. Jeitschko, M. H. Gerss, J. Less-Common Met. **116**, 147 (1986).
[6] U. Jakubowski-Ripke, W. Jeitschko, J. Less-Common Met. **136**, 261 (1988).
[7] W. Jeitschko, L. J. Terbüchte, E. J. Reinbold, P. G. Pollmeier, T. Vomhof, J. Less-Common Met. **161**, 125 (1990).
[8] H. Kleinke, H. F. Franzen, J. Solid State Chem. **137**, 218 (1998).
[9] R. Pöttgen, H. Borrmann, C. Felser, O. Jepsen, R. Henn, R. K. Kremer, A. Simon, J. Alloys Compd. **235**, 170 (1996).
[10] B. Ya. Kotur, E. Gratz, Scandium Alloy Systems and Intermetallics, in K. A. Gschneider (Jr.), L. Eyring (eds.): Handbook on the Physics and Chemistry of Rare Earths, Vol. 27, chapter 175, Elsevier, Amsterdam (1999).
[11] V. I. Zaremba, V. M. Baranyak, Ya. M. Kalychak, Vestn. Lvov Univ., Ser. Khim. **25**, 18 (1984).
[12] N. N. Kiseleva, Izv. Akad. Nauk. SSSR, Metally **2**, 213 (1987).
[13] A. E. Dwight, C. W. Kimball, J. Less-Common Met. **127**, 179 (1987).
[14] B. T. Matthias, E. Corenzwit, J. M. Vandenberg, H. Barz, M. B. Maple, R. N. Shelton, J. Less-Common Met. **46**, 339 (1976).
[15] R. Pöttgen, R. Dronskowski, Z. Anorg. Allg. Chem. **622**, 355 (1996).
[16] F. Hulliger, J. Alloys Compd. **232**, 160 (1996).
[17] Ya. V. Galadzhun, V. I. Zaremba, H. Piotrowski, P. Mayer, R.-D. Hoffmann, R. Pöttgen, Z. Naturforsch. **55b**, 1025 (2000).
[18] V. P. Urvachev, V. P. Polyakova, E. M. Savitskii, in: Splavy Redk. Met. Osobymi Fiz. Svojstvami: Redkozem. Blagorodn. Met. 141 (1983).
[19] R. Pöttgen, Th. Gulden, A. Simon, GIT Labor-Fachzeitschrift **43**, 133 (1999).
[20] K. Yvon, W. Jeitschko, E. Parthé, J. Appl. Crystallogr. **10**, 73 (1977).
[21] G. M. Sheldrick, SHELXL-97, Program for Crystal Structure Refinement, University of Göttingen, Germany (1997).
[22] H. D. Flack, G. Bernadinelli, Acta Crystallogr. A **55**, 908 (1999).
[23] H. D. Flack, G. Bernadinelli, J. Appl. Crystallogr. **33**, 1143 (2000).
[24] H. Bärnighausen, Commun. Math. Chem. **9**, 139 (1980).

[25] H. Bärnighausen, U. Müller, Symmetriebeziehungen zwischen den Raumgruppen als Hilfsmittel zur straffen Darstellung von Strukturzusammenhängen in der Kristallchemie, University of Karlsruhe and University/GH Kassel, Germany (1996).
[26] S. Rundqvist, F. Jellinek, Acta Chem. Scand. **13**, 425 (1959).
[27] J. T. Zhao, E. Parthé, Acta Crystallogr. **C46**, 2273 (1990).
[28] E. Parthé, L. Gelato, B. Chabot, M. Penzo, K. Cenzual, R. Gladyshevykii, TYPIX – Standardized data and crystal chemical characterization of inorganic structure types. Gmelin Handbook of inorganic and organometallic chemistry, 8th edition, Springer, Berlin (1993).
[29] M. F. Zumdick, R. Pöttgen, Z. Kristallogr. **214**, 90 (1999).
[30] P. I. Krypyakevich, V. Ya. Markiv, E. V. Melnyk, Dopov. Akad. Nauk. Ukr. RSR, Ser. A 750 (1967).
[31] A. E. Dwight, M. H. Mueller, R. A. Conner, Jr., J. W. Downey, H. Knott, Trans. Met. Soc. AIME **242**, 2075 (1968).
[32] M. F. Zumdick, R.-D. Hoffmann, R. Pöttgen, Z. Naturforsch. **54**, 45 (1999).
[33] V. I. Zaremba, Ya. M. Kalychak, P. Yu. Zavalii, A. N. Sobolev, Dopov. Akad Nauk Ukr. RSR, Ser. B 38 (1989).
[34] M. F. Zumdick, G. A. Landrum, R. Dronskowski, R.-D. Hoffmann, R. Pöttgen, J. Solid State Chem. **150**, 19 (2000).
[35] M. F. Zumdick, R. Pöttgen, V. I. Zaremba, R.-D. Hoffmann, J. Solid State Chem. **166**, 305 (2002).
[36] M. Lukachuk, V. I. Zaremba, R. Pöttgen, Intermetallics **11**, 581 (2003).
[37] J. Donohue, The Structures of the Elements, Wiley, New York (1974).